Reaction calorimetry as an in-situ kinetic tool for characterizing complex reactions [1]

C. LeBlond [a], J. Wang [a], R.D. Larsen [a], C.J. Orella [a], A.L. Forman [a],
R.N. Landau [a,1], J. Laquidara [b], J.R. Sowa, Jr. [b]
D.G. Blackmond [a,2], Y.-K. Sun [a,*].

[a] *Merck Research Laboratories, Merck & Co., Inc., P.O. Box 2000, RY55-228, Rahway, NJ 07065*
[b] *Department of Chemistry, Seton Hall University, South Orange, NJ 07079*

Abstract

Due to its ability to provide directly reaction rate data and its in-situ nature, reaction calorimetry has become one of the most powerful probes of reaction pathways and mechanisms of chemical reactions by virtue of providing high-quality kinetic data. In this paper, examples of enantioselective hydrogenation and selective consecutive hydrogenation reactions are presented to demonstrate the high quality of kinetic data obtainable from the reaction calorimetry. They are also used to illustrate the use of reaction calorimetry for elucidating reaction pathways and mechanisms from detailed kinetic and thermodynamic information about individual step involved in multi-step reactions that is otherwise difficult to obtain without calorimetry.

1. Introduction

Calorimetry is hardly a new technique. One often thinks of thermodynamics when one thinks of calorimetry since it has long been used to determine thermodynamic properties of materials and chemical processes. However, only with the advent of

---

* Corresponding author.
[1] This paper is a contribution to the special thematic issue "Reaction Calorimetry", edited by Ralph N. Landau.
[2] Current Address: Sandoz Pharmaceuticals Corp., 59 Route 10, East Hanover, NJ 07936.
[3] Current Address: Max-Planck Institut für Kohlenforschung, Mülheim, an-der-Ruhr, Germany.

automated reaction calorimeters, such as Mettler's Reaction Calorimeter, which can measure the rate of heat flow into or out of a reactor during a reaction while maintaining precise control of the temperature of the contents in the reactor, did calorimetry begin to be employed for kinetic studies of chemical processes, including pharmaceutical and fine chemical reactions and process development (1,2).

This paper first offers a brief comparison of various methods of monitoring kinetics of chemical reactions (Sec. 2), from which it will be clear that reaction calorimetry stands out as one of the most powerful tools for kinetic studies of chemical processes. It will be demonstrated (Sec. 3) using four examples that heat flow from reaction calorimetry can provide high quality kinetic data which can shed light on reaction mechanisms, help evaluation of proposed reaction intermediates and reaction pathways, and make it possible to extract kinetic and thermodynamic data associated with each individual step involved in the reaction.

2. Advantages of calorimetry as a kinetic tool

Accurate measurement of kinetics is essential for investigation of reaction mechanisms, since kinetics are a "reflection" of the reaction mechanism. From a practical point of view, it is also essential to have a complete picture of the reaction kinetics for successful process development and optimization.

According to the types of data obtained, methods for measurement of kinetics may be classified into two categories. The first category provides information on concentrations and conversion, or integral properties, since they measure integration of variables such as rate from the beginning of the reaction to the point of measurement. To obtain rate, one has to differentiate these integral results with respect to time. Obviously, an accurate determination of rate from these integral properties requires high rates of sampling.

The most commonly used method for monitoring kinetics of synthetic organic reactions is direct sampling from then reactor followed by chemical analysis. While this method is valuable in providing concentration, or conversion information, and in particular, chemical identities of components in the reactor, it has a three-fold deficiency insofar as a determination of kinetics is concerned. First, only integral properties (e.g., concentration) are measured. Second, in reality, only a limited number of samples may be taken per reaction, a factor that makes it highly inaccurate to determine instantaneous rate by differentiating the concentration data with respect to time. Finally, it is not an in-situ method. The sample has to be taken away from the reacting atmosphere for work-up and analysis, during which period the sample may undergo chemical changes, thus distorting the true profile of components in the reactor.

Other integral methods include in-situ spectroscopic techniques, such as time-resolved infrared spectroscopy which measures concentration or conversion as well as provides information on chemical identities of components in the reactor. In contrast to the chemical sampling method, the IR spectrum of the reacting system may be collected at a much faster pace than that normally possible for the chemical sampling method. Consequently, rate data may be derived with good accuracy by differentiating the IR intensity data with respect to time.

The second category of methods is characterized by direct measurement of differential properties such as the instantaneous rate of the reaction. Reaction calorimetry, representing this category of methods, is a much more powerful method for monitoring kinetics. Modern reaction calorimetry keeps track of the flow rate of heat into and out of the reactor by the chemical processes inside the reactor while maintaining precise control of the temperature of the contents in the reactor according to a user-defined temperature profile. The heat flow rate measured under isothermal conditions is directly proportional to a summation of the rate of each reaction step as weighed by heat of reaction ΔH_i of the corresponding step, i.e.,

$$q_r = V_r \sum_i \Delta H_i \left(\frac{\mathrm{d}C_i}{\mathrm{d}t}\right),$$　　　(1)

where V_r is the volume of the contents in the reactor, ΔH_i, is the heat of reaction for the ith step. In addition to measuring directly the differential properties i.e., rate of the chemical reaction, the reaction calorimetry conducts the measurements in an in-situ, non-invasive, on-line, and quasi-continuous fashion, which is difficult, if not impossible, to achieve using the chemical sampling method. While the chemical sampling method is most valuable in providing information on the chemical identities of components in the reactor, it is not an accurate kinetic tool. The salient advantages of the reaction calorimetry may make up for this obvious shortcoming of the chemical sampling method in such a way that accurate measurements of kinetics may be achieved. A combined approach from both the heat flow measurement using reaction calorimetry and from the chemical sampling method would enable one to obtain a complete picture of kinetics and reaction pathways associated with a chemical reaction.

3. Clear pictures of reaction kinetics revealed by calorimetry

Four examples are given below to illustrate the quality of the kinetic data obtainable from the reaction calorimetry and information that may be extracted from it. All four examples are catalytic hydrogenation reactions, both homogeneous and heterogeneous. Obviously, the calorimetric technique is not limited by hydrogenation only, but is applicable to any process that has a heat effect associated with it. The advantage of using hydrogenation reactions as examples is that rate of hydrogen uptake, which is proportional to the rate of each reaction step occuring in the reactor by

$$R_{\mathrm{H_2}} = V_r \sum_i \Delta N_i \left(\frac{\mathrm{d}C_i}{\mathrm{d}t}\right),$$　　　(2)

where ΔN_i is the hydrogen stoichiometry for the ith hydrogenation step, may be recorded continuously in parallel to the heat flow rate. The hydrogen uptake rate profile can be used as a check to confirm the accuracy of the reaction rate measured by the heat flow, and to provide additional insights into the hydrogenation pathways. In addition, for a hydrogenation reaction, a combination of the hydrogen uptake data and

the heat flow data yields direct information on thermodynamic data associated with each steps in a multi-step hydrogenation reaction, as will be shown below.

3.1. Heterogeneously-catalyzed enantioselective hydrogenation of ethyl pyruvate

Chiral hydrogenation of ethyl pyruvate on Pt containing chiral surface modifiers, i.e.,

Ethyl Pyruvate   (S)-Ethyl Lactate   (R)-Ethyl Lactat
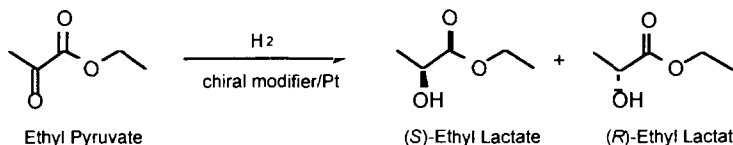
has received significant attention in the literature because it represents one of the few successful examples of asymmetric hydrogenation over a heterogeneous catalyst. One striking observation is that with dihydrocinchonidine as a chiral surface modifier, enantiomeric excess of (R)-ethyl lactate, defined as

$$ee = \frac{[R] - [S]}{[R] + [S]},$$ (3)

increases initially with time (Fig. 1) (3,4). Toward an understanding of the nature of the modification of the Pt surface by chiral modifiers, an accurate measurement of reaction kinetics is essential. A typical conversion profile determined from periodic sampling from the reactor followed by GC analysis is displayed in Fig. 1. An accurate determination of the rate during this "chiral induction" period from Fig. 1 would be difficult because one has to differentiate the limited number of conversion data with respect to time. The reaction calorimetry, however, offers a clear picture of what happens to the kinetics of the hydrogenation during this period.

Fig. 2 shows the heat flow data recorded simultaneously with the chemical analysis data shown in Fig. 1. It reveals an important aspect of the reaction mechanism: concomitant with the increase of enantioselectivity during the initial period of reaction, there was a rate acceleration: the rate of hydrogenation increases with time or decreasing concentration of ethyl pyruvate in the liquid phase. The rate acceleration was only observed in the presence of dihydrocinchonidine without which the rate of hydrogenation simply decayed monotonously.

The rate profile of hydrogen uptake, which serves as a true measure of the rate of hydrogenation of ethyl pyruvate, is also shown in Fig. 2 together with the heat flow data. The fact that the heat flow profile agrees completely with the hydrogen uptake rate data, particularly in the region where the rate increases with time, confirms that the heat flow data reflect only as well as accurately kinetics of the hydrogenation reaction.

The rate acceleration in Fig. 2 shown by calorimetry is difficult to discern from the conversion data obtained from GC analysis of the samples periodically taken from the reactor. This demonstrates clearly the power of calorimetry as a kinetic tool in revealing fine details of the reaction kinetics. The usefulness of the reaction calorimetry
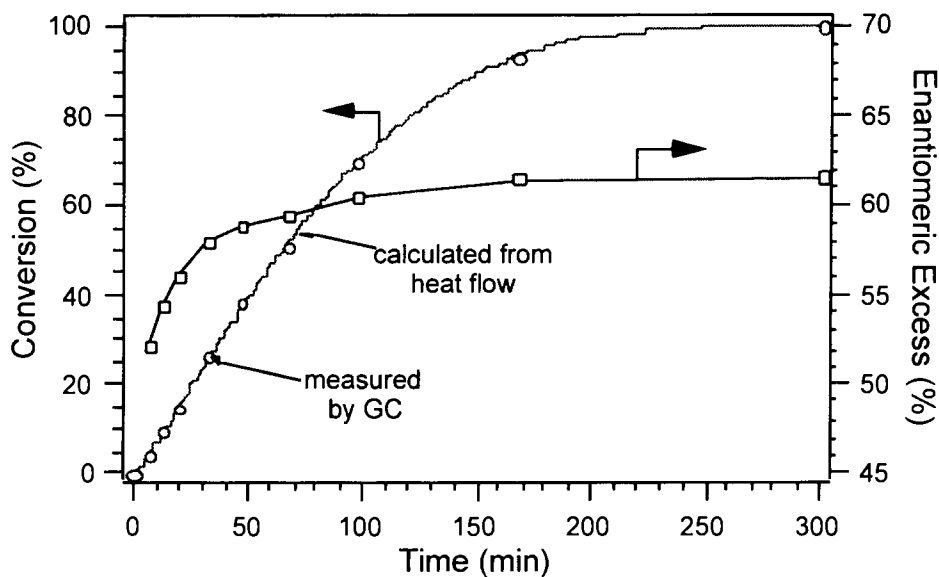
Fig. 1. Conversion and enantiomeric excess as a function of time during isothermal hydrogenation of ethyl pyruvate over dihydrocinchonidine-modified Pt/Al_2O_3. The solid line that goes through the conversion data is calculated from the heat flow data using Eq. 4. [ethyl pyruvate]$_0$ = 1 M, solvent: n-propanol, 283 K, H_2 pressure = 70 psig.
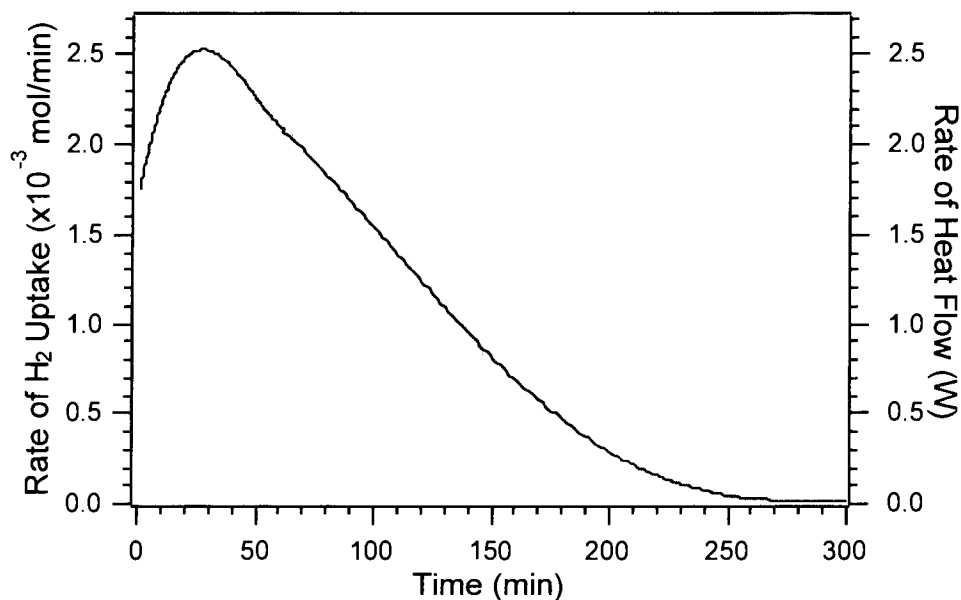

Fig. 2. Rate of heat flow (dot) and rate of hydrogen uptake (line) as a function of time, recorded simultaneously with the chemical analysis data shown in Fig. 1 during the isothermal hydrogenation of ethyl pyruvate over dihydrocinchonidine-modified Pt/Al_2O_3.

is further demonstrated by predicting the integral properties such as conversion of the substrate via calculating the fractional heat evolution (FHE) using Eq. 4:

$$conversion = FHE = \int_0^t q_r\,\mathrm{d}t \Big/ \int_0^\infty q_r\,\mathrm{d}t. \tag{4}$$

Conversion calculated from the heat flow curve in Fig. 2 is shown in Fig. 1 as the solid line. It is in excellent agreement with the results from chemical analysis of the samples taken from the reactor over the course of the reaction.

How the observed rate acceleration is related to the rise in enantioselectivity is not entirely clear, but it may be related to an *in-situ* reaction-driven modification of the catalytic surface for enantioselective hydrogenation (3), which also enhances rate of hydrogenation. Fine details of kinetics such as the rate acceleration observed here offer hints on the mechanism. The rising rate observed with reaction calorimetry provides a criteria for testing any proposed mechanism for the *in-situ* reaction-driven chiral modification of the catalytic surface.

3.2. Catalytic hydrogenation of 1-(4-Nitrobenzyl)-1,2,4- triazole

3.2.1. Kinetics

Fig. 3 shows kinetics, as measured by heat flow, of the selective hydrogenation of 1-(4-nitrobenzyl)-1,2,4-triazole (4NBT) over Pd/C at 25°C to its aniline equivalent, 1(-4-aminobenzyl)-1,2,4-triazole, i.e.,
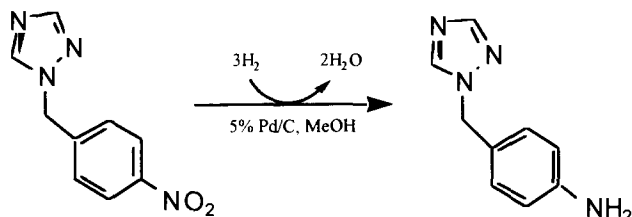
The heat flow profile shows clearly that there are two distinct kinetic regimes with an abrupt transition between them. As a comparison, rate of hydrogen uptake is also shown in Fig. 3. The general characteristics of the kinetics agree well, such as the quasi zero-order kinetics in the first regime, and the sharp transition between the two regimes. This shows that the heat flow indeed provides an accurate picture of the kinetics of the hydrogenation reaction.

3.2.2. Reaction pathway

The presence of two very different kinetic regimes, as indicated by the heat flow profile, immediately suggests that two different chemical processes are occuring at these two regimes, provided that the catalyst is not de-activated. Indeed, chemical analysis of components from batch samples taken during reaction (Fig. 4) shows that the first kinetic regime corresponds to hydrogenation of 4NBT to a hydroxylamine
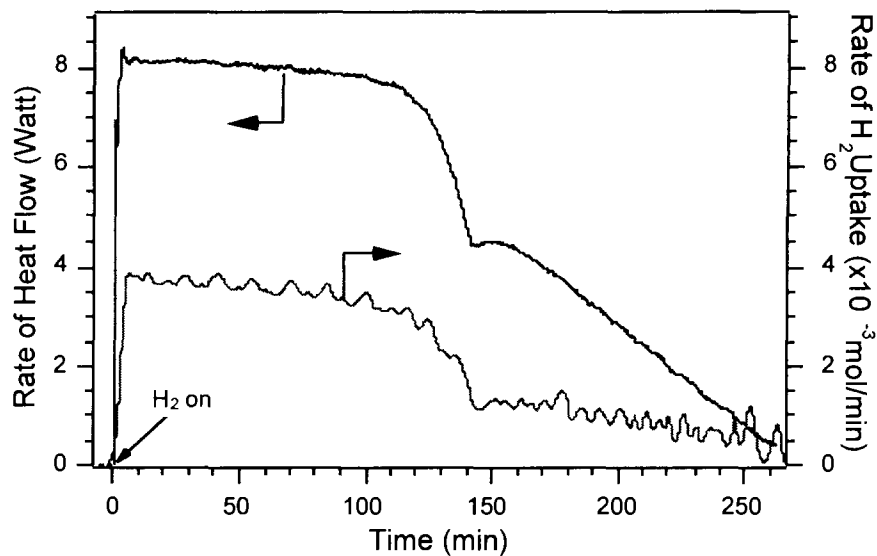
Fig. 3. Rates of heat flow and hydrogen uptake for isothermal (25°C) hydrogenation of 1-(4-nitrobenzyl)-1,2, 4-triazole to 1-(4-aminobenzyl)-1, 2, 4-triazole over Pd/C in methanol.
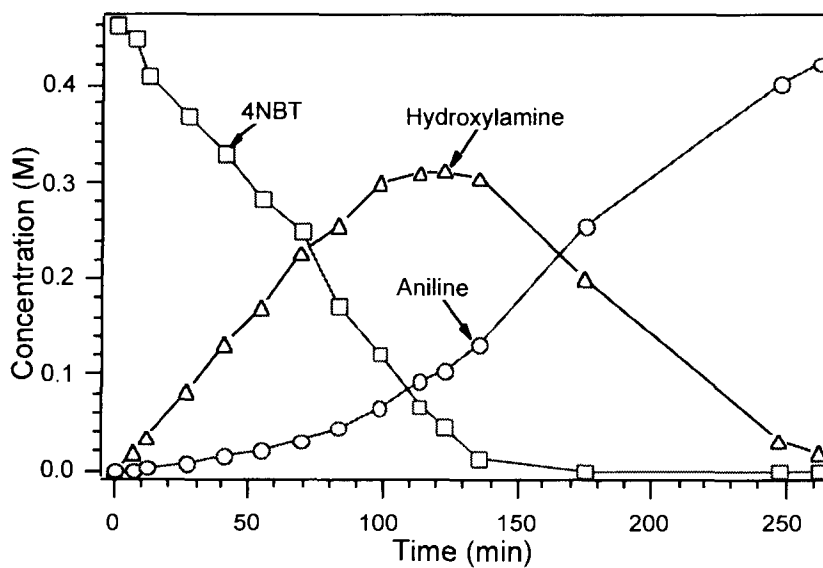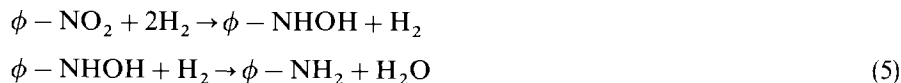

Fig. 4. Profile of components in the reactor corresponding to the heat flow curve in Fig. 3. Determined by sampling from reactor followed by HPLC analysis.

intermediate, whereas the second corresponds to the subsequent hydrogenation of the hydroxylamine to the aniline product, i.e.,

$$\phi - NO_2 + 2H_2 \rightarrow \phi - NHOH + H_2$$

$$\phi - NHOH + H_2 \rightarrow \phi - NH_2 + H_2O \tag{5}$$

For this consecutive hydrogenation reaction, the rate of heat flow does not simply correspond to the rate of concentration change of the substrate 4NBT. Rather, it is a summation of rate of concentration changes of the substrate and hydrogenation intermediates as weighed by the corresponding heat of hydrogenation, ΔH_i (Eq. 2). Hence, conversion of the substrate in this case may not be as easily determined from the heat flow curve using the fractional heat evolution (Eq. 4) as in the case discussed in Sec. 3.1.

3.2.3. Stepwise thermodynamics

The overall heat of hydrogenation from 4NBT to the aniline can be conveniently calculated to be -127 ± 4 kcal/mol by integrating the heat flow rate curve in Fig. 3, in good agreement with the value for hydrogenation of nitrobenzene to aniline. As will be shown below, the stepwise heats of hydrogenation of this two-step consecutive hydrogenation reaction may also be determined from a combination of the heat flow data and the hydrogen uptake data.

Instantaneous heat of hydrogenation per mol of hydrogen reacted, ΔH_{H_2}, defined as (using Eqs. 1 and 2)

$$\Delta H_{H_2} = \frac{q_r}{R_{H_2}} = \frac{\sum_i \Delta H_i \left(\dfrac{dC_i}{dt} \right)}{\sum_i \Delta N_i \left(\dfrac{dC_i}{dt} \right)}, \tag{6}$$

can be obtained by dividing a heat flow curve by the corresponding reactive hydrogen uptake curve. Due to the sequential nature, the heat flow at the initial stage of the reaction may be attributed mainly to the hydrogenation of 4NBT to the hydroxylamine, whereas at the final stage mainly to the hydrogenation of the hydroxylamine to the aniline. At these two extremes, Eq. 6 becomes simplified to yield thermodynamic information for each individual step involved in the hydrogenation reaction. At the early stage of the reaction, since

$$\frac{dC_1}{dt} \gg \frac{dC_2}{dt},$$

Eq. 6 becomes

$$\Delta H_{H_2} \approx \frac{\Delta H_1}{\Delta N_1}.$$

At the final stage of the reaction, since

$$\frac{dC_2}{dt} \gg \frac{dC_1}{dt},$$

Eq. 6 becomes

$$\Delta H_{\text{H}_2} \approx \frac{\Delta H_2}{\Delta N_2}.$$

The instantaneous heat of hydrogenation per mol of hydrogen reacted obtained from Fig. 3 according to Eq. 6 is displayed in Fig. 5. Corresponding to the two distinct kinetic regimes in the hydrogenation kinetics (Fig. 3), there are also two distinct regimes in the heat of hydrogenation, with the transition occuring at the same time.

At the initial stage of the first regime, ΔH_{H_2} was ~ -32.5 kcal/mol$_-$H$_2$, whereas in the second regime it increased to ~ -58 kcal/mol$_-$H$_2$. For the first step in the reaction pathway (Eq. 5), because the hydrogen stoichiometry is two ($\Delta N_1 = 2$) for hydrogenation of 4NBT to the hydroxylamine, the heat of hydrogenation shown in Fig. 5 at the beginning of the first regime (-32.5 kcal/mol$_-$H$_2$) corresponds to half of ΔH_1. In other words, $\Delta H_1 = -65$ kcal/mol. Similarly, because the hydrogen stoichiometry is one ($\Delta N_2 = 1$) for the second step from the hydroxylamine to the aniline, the heat of hydrogenation shown in Fig. 5 in the second regime (-58 kcal/mol) equals ΔH_2. Heat of hydrogenation from 4NBT to the aniline is a sum of these two stepwise heats, i.e., -123 kcal/mol. These thermodynamic results are summarized in Table 1 and in a one-dimensional potential energy diagram in Fig. 6.

As a hydrogenation intermediate, the hydroxylamine is rather unstable. It undergoes facile oxidation reaction in the presence of air to dimerize into the azoxy compound. As
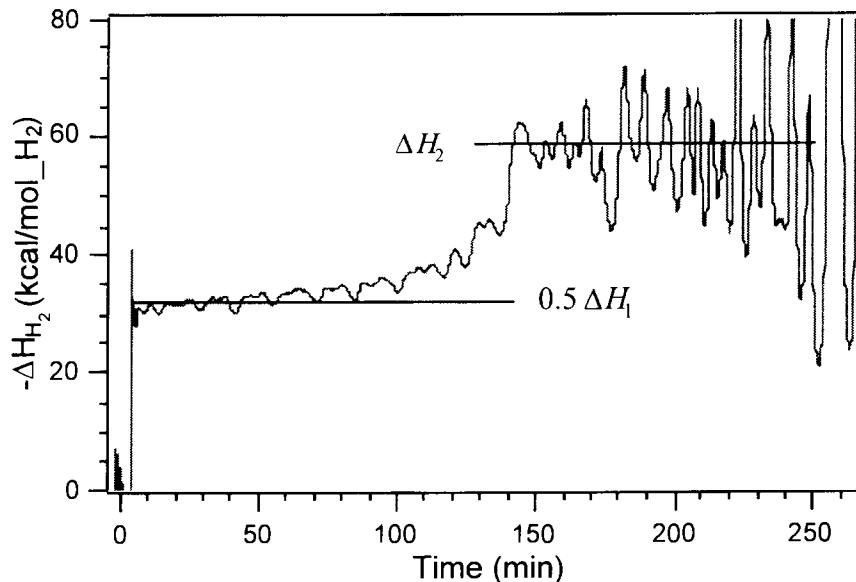

Fig. 5. Instantaneous heat of hydrogenation for each mol of hydrogen reacted as a function of time. Derived using Eq. (6) by taking the ratio of the heat flow curve to the reactive hydrogen uptake curve in Fig. 3.

Table 1

Step-wise heats of hydrogenation for hydrogenation of the nitro group in 1-(4-nitrobenzyl)-1, 2, 4-triazole

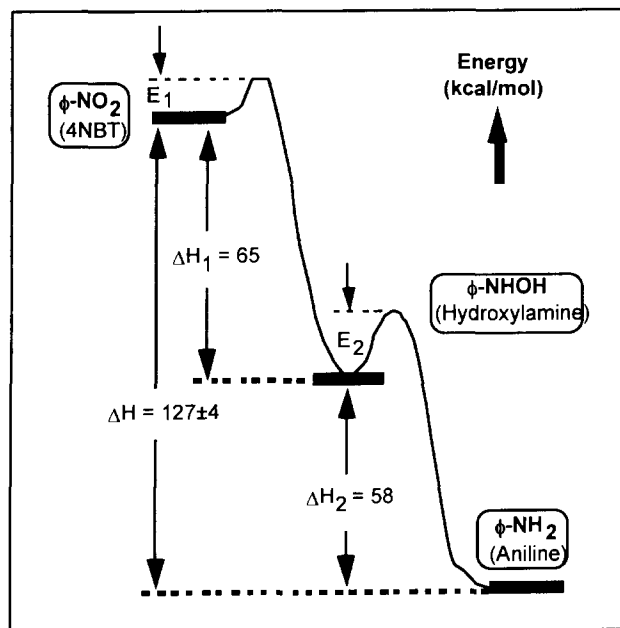| Hydrogenation Reaction	Heat of Hydrogenation, ΔH, (kcal/mol)
$\phi - NO_2 + 2H_2O \rightarrow \phi - NHOH + H_2$	-65
$\phi - NHOH + H_2 \rightarrow \phi - NH_2 + H_2$	-58

Fig. 6. One-dimensional potential energy diagram that depicts thermodynamics associated with the step-wise hydrogenation of 1-(4-nitrobenzyl)-1, 2, 4-triazole.

a result, a direct determination of its heat of formation may be difficult. The heat of formation of the unstable hydroxylamine, however, is implicit in the stepwise heats of hydrogenation determined above. The results on the calculated heats of formation are listed in Table 2.
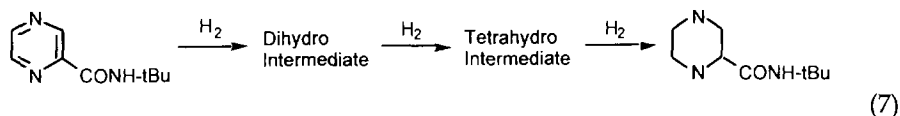
Table 2

Heat of formation, ΔH_f (kcal/mol, relative to that of 4NBT), of species associated in hydrogenation of 1-(4-nitrobenzyl)-1,2,4-triazole.

1-(4-nitrobenzyl-1,2,4-triazole (4NBT)	the hydroxylamine Intermediate	the aniline product
0	-0.69	9.63

3.3. Catalytic hydrogenation of pyrazine-2-t-butylcarboxamide to piperazine-2-t-butylcarboxamide

Another example of consecutive hydrogenation is the hydrogenation reaction of pyrazine-2-t-butylcarboxamide to piperazine-2-t-butylcarboxamide, an intermediate of Merck's AIDS protease inhibitor Crixivan®:

$$\text{pyrazine} \xrightarrow{H_2} \text{Dihydro Intermediate} \xrightarrow{H_2} \text{Tetrahydro Intermediate} \xrightarrow{H_2} \text{piperazine}$$

(7)

This example will show how the results from reaction calorimetry can be utilized to identify hydrogenation intermediates and help determine the hydrogenation pathway.

The reaction kinetics, measured by heat flow during hydrogenation over a Pd/C catalyst at 35°C are in good agreement with the rate of hydrogen uptake data recorded simultaneously (Fig. 7). There were also two distinct kinetic regimes: one fast ($t < 50$ min) and the other slow ($t > 50$ min). In fact, at 35°C, the rate in the second regime was so slow that the heat flow was barely measurable. The kinetic picture suggested by the calorimetry shows the reaction pathway is composed of two kinetically distinguishable steps. Results from GC analysis of samples taken during the course of the reaction (Fig. 8) indicate that there is a significant buildup of an intermediate in the liquid phase. The manner with which the concentrations of the starting pyrazine, the intermediate,
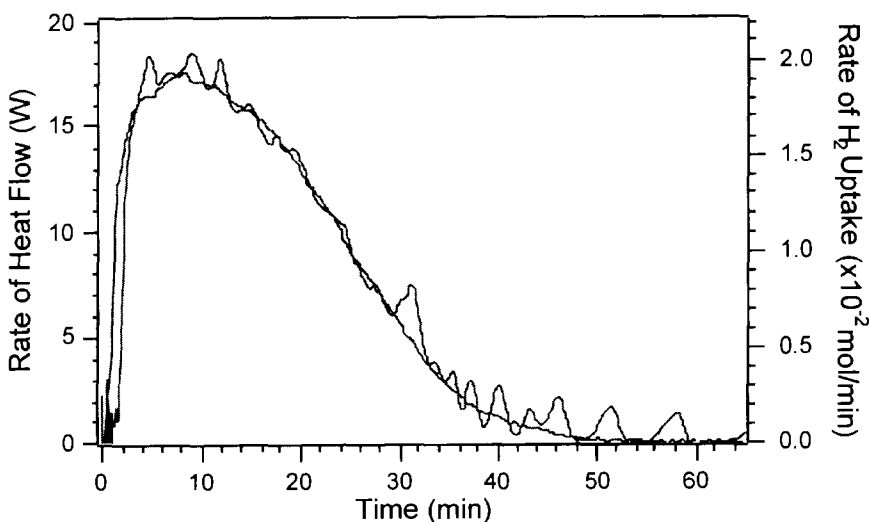

Fig. 7. Overall rate of hydrogenation as measured by the rated heat flow (solid line) and H_2 uptake (dash line) during hydrogenation of pyrazine-2-*t*-butylcarboxamide at 35°C and 70 psig H_2 over a *Pd/C* catalyst.
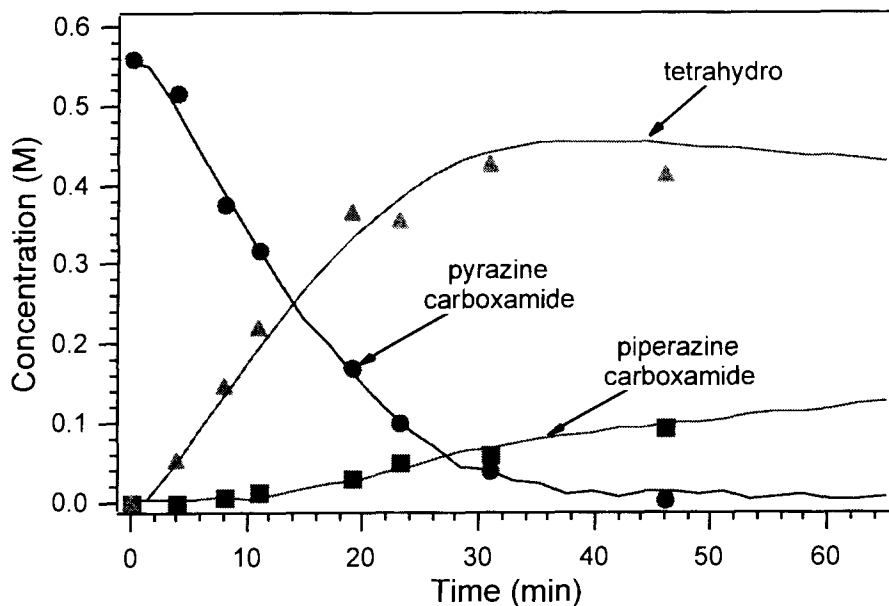
Fig. 8. Concentration profiles of components in the reactor during hydrogenation. Corresponds to the kinetics in Fig. 7.

and the product change with time shows that these two steps are sequential, namely, the fast kinetic regime corresponds mainly to hydrogenation of the starting pyrazine to this intermediate, and the slow regime mainly to the hydrogenation of the intermediate to the piperazine. As to the identity of the intermediate, there are two possibilities, it could either be the dihydro or the tetrahydro species (Eq. 7).

Due to the sequential nature of the reaction, the beginning stage of the first kinetic regime corresponds nearly exclusively to the first step of the two-step consecutive reaction, i.e., hydrogenation of the pyrazine substrate to the intermediate (Fig. 8). Hence, the heat of hydrogenation associated with the first step on a molar basis of starting pyrazine reacted as well as on a molar basis of hydrogen reacted may be determined. Fig. 9 shows that the heat of hydrogenation for each mol of the starting pyrazine is ~ -26 kcal/mol$\_$pyrazine. Fig. 10 shows that the corresponding heat of hydrogenation per mol of hydrogen reacted, ΔH_{H_2}, is -13 kcal/mol$\_$H$_2$, almost precisely one half of the heat of hydrogenation per mol of the starting pyrazine. These results indicate that the first step which leads to the formation of the intermediate has a hydrogen stoichiometry of two. Consequently, it may be concluded that the hydrogenation intermediate is the tetrahydro species, in good agreement with results from NMR analysis of the intermediate (6).

In a separate experiment carried out at 60°C where the pyrazine was completely hydrogenated to the pyperazine, heat of hydrogenation from the pyrazine to the pyperazine was determined to be -46 kcal/mol, in good agreement with a previously measured value (2). Thus, the heat of hydrogenation from the tetrahydro intermediate
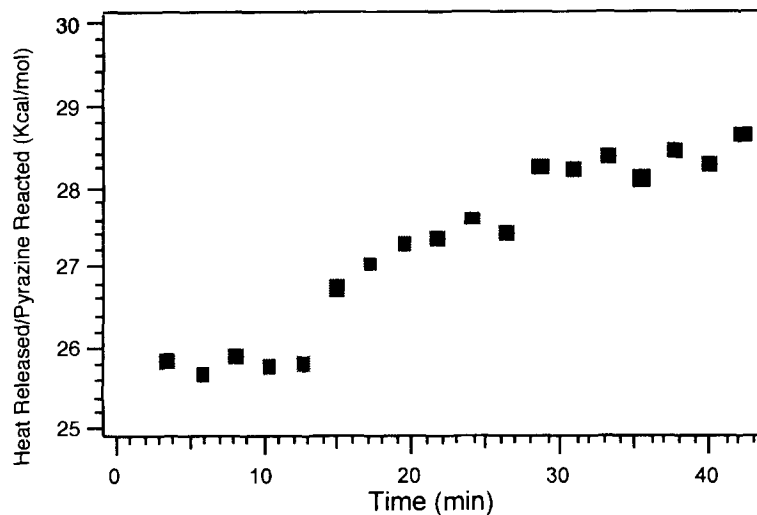
Fig. 9. Heat released divided by moles of the pyrazine reacted as a function of time. Derived from the heat flow data in Fig. 7 and the GC analysis data in Fig. 8.
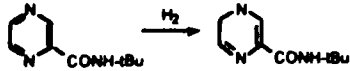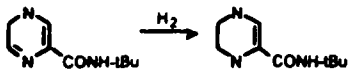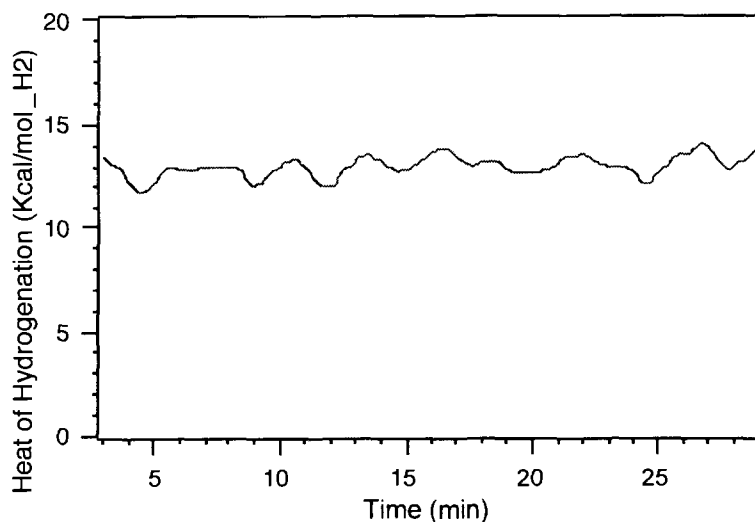

Fig. 10. Instantaneous heat of hydrogenation for each mol of hydrogen reacted, ΔH_{H_2}, as a function of time. Derived from Eq. (6) by taking the ratio of the heat flow curve to the reactive hydrogen uptake curve in Fig. 7. Note that only data in the first kinetic regime are displayed.

to the piperazine product may be calculated to be -20 kcal/mol. Results on the stepwise heats of hydrogenation are summarized in Table 3. In comparison with results from a semi-empirical quantum mechanical calculation (6) also listed in Table 3, the agreement between them is excellent. For example, the calculated heat of hydrogena-

Table 3
Summary of calculated and experimental heats of hydrogenation in hydrogenation of pyrazine-2-t-butylcarboxamide to pyperazine-2-t-butylcarboxamide

Hydrogenation Reaction	Heat of Hydrogenation, ΔH_i, (kcal/mol)	
	Calculated*	Experimental
(pyrazine-2-t-butylcarboxamide) $\xrightarrow{H_2}$ (dihydro)	-9.9	-26
(dihydro) $\xrightarrow{H_2}$ (tetrahydro)	-17.7	
(tetrahydro) $\xrightarrow{H_2}$ (pyperazine-2-t-butylcarboxamide)	-20.6	-20

* Calculated from a semi-empirical quantum mechanical package MOPAC with AM1 (2).

tion from pyrazine to the tetrahydro species is -27.6 kcal/mol, as compared with the experimental value of -26 kcal/mol.

The good agreement between the calculated and experimental values of the stepwise heats of hydrogenation opens another avenue for identification of hydrogenation intermediates. For an unidentified hydrogenation intermediate, a comparison of its heat of hydrogenation determined experimentally with values calculated for a number of proposed intermediates helps to discriminate between the proposed intermediates and thus the proposed pathways. In the case discussed above, the measured heat of hydrogenation from the starting pyrazine to the intermediate (-26 kcal/mol) is far different from the value for the dihydro species (-9.9 kcal/mol) but almost equals the value calculated for the tetrahydro species (-27.6 kcal/mol). In addition, ΔH_{H_2} was -13 kcal/mol $\_$ H_2, far greater than the value of -9.9 kcal/mol calculated for the dihydro species. Both facts support the conclusion that the intermediate is the tetrahydro species.

An interesting issue for this reaction was the question regarding whether the dihydro intermediate is present to any substantial degree under any other reaction conditions, particularly at low temperatures when the dihydro is most likely to accumulate in the solution. Although the dihydro could not be observed by GC, its presence as an intermediate in the reactor may not be excluded due to its great instability outside the reactor. Thus, reaction calorimetry, as an in-situ monitor, can help greatly in answering this question by providing ΔH_{H_2} at the beginning stage of the reaction, which can be compared with the calculated value for the dihydro species. For experiments carried out from $60°C$ to at as low as $5°C$, ΔH_{H_2} at the beginning stage of the reaction was consistently -13 kcal/mol $\_$ H_2, which is nearly 50% of the value calculated for the

tetrahydro species, but far greater than the value of -9.9 kcal/mol expected for hydrogenation of the pyrazine to the dihydro. These results indicate that there was not any substantial amount of dihydro present during the hydrogenation reactions under these conditions, most likely due to high hydrogenation reactivity of the dihydro species on the catalytic surface to the tetrahydro intermediate.

A determination of the stepwise heats of hydrogenation leads to a determination of the heat of formation of the rather unstable tetrahydro hydrogenation intermediate. The results are shown in Table 4.

3.4. Asymmetric hydrogenation of geraniol

A striking observation made during $[RuCl_2((S)-(-)-tol-binap)]_2 \cdot N(C_2H_5)_3$ catalyzed asymmetric hydrogenation of geraniol

| Geraniol | | (S)-β-Citronellol | (R)-β-Citronellol |
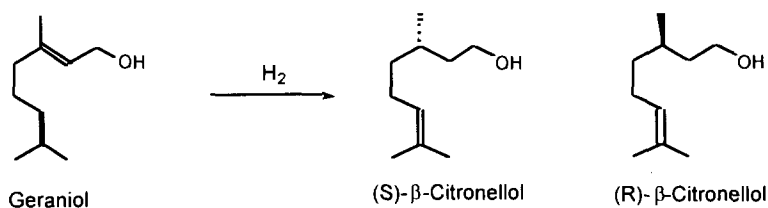
was the unusual heat flow curve shown in Fig. 11. The heat flow curve shows that there are two distinct kinetic regimes. The rate of hydrogenation in the first regime ($t < 15$ min.) is much faster than that in the second regime ($t > 15$ min.). Transition between these two kinetic regimes is extremely abrupt. The accuracy of the heat flow as a measure of hydrogenation rate was confirmed by the rate of hydrogen uptake (also shown in Fig. 11) measured simultaneously.

An even more striking observation was that there was a marked shift in the enantiomeric excess from $\sim 85\%$ ee to (S)-citronellol at the beginning stage of the reaction to over 40% ee to (R)-citronellol at high conversion (5). This inversion of enantiomeric excess during the course of the hydrogenation reaction is shown in Fig. 12 where the cumulative enantiomeric excess measured by GC is plotted as a function of conversion.

The two distinct heat flow regimes with an abrupt transition between them immediately suggested two different hydrogenation reactions involving two different substrates. But what would the two substrates be when geraniol was the only substrate charged (with the catalyst) into the reactor? Fig. 11 shows that one substrate was hydrogenated

Table 4
Heat of formation, ΔH_f (kcal/mol, relative to that of the pyrazine starting material), of species involved in hydrogenation of pyrazine-2-t-butylcarboxamide

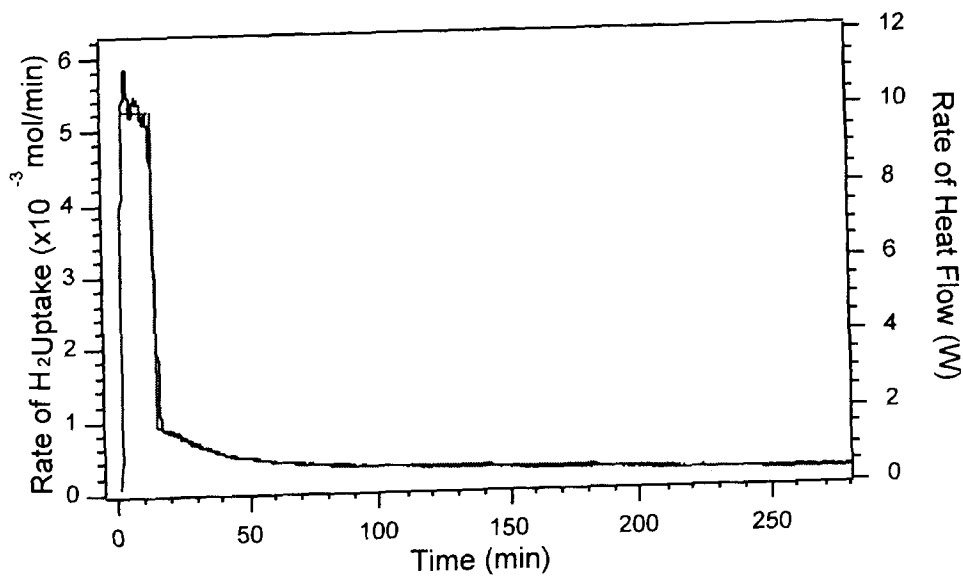| pyrazine 2-t-butylcarboxamide	tetrahydro Intermediate	the pyperazine product
0	-26	-46

Fig. 11. Heat flow curve during $[RuCl_2((S)-(-)-tol-binap)]_2 \cdot N(C_2H_5)_3$ catalyzed asymmetric hydrogenation of geraniol in methanol at 20°C and 60 psig. Also plotted is rate of hydrogen uptake profile. The agitation speed was 400 rpm.
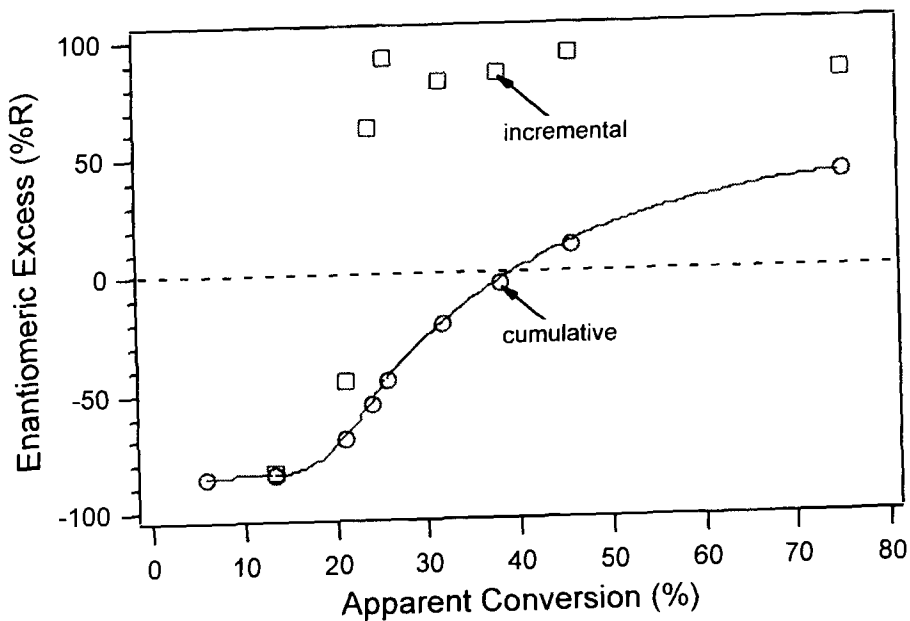

Fig. 12. Cumulative and incremental enantiomeric excess as a function of conversion of geraniol determined by GC during $[RuCl_2((S)-(-)-tol-binap))]_2 \cdot N(C_2H_5)_3$ catalyzed hydrogenation of geraniol at 293 K and 60 psig.

with much faster rate than the other under the same conditions. Furthermore, the virtually identical instantaneous heats of hydrogenation per mol of H_2 reacted (calculated from the heat flow data and rate of hydrogen uptake data in Fig. 11 using Eq. 6) in these two regimes suggested that these two substrates could be isomers. This prompted us to look more closely at the composition of components in the reactor prior to and following pressurization with hydrogen. It was found by GC that before hydrogen was applied, there were indeed two substrates in the reactor (see composition at $t = 0$ in Fig. 13), one was geraniol and the other γ-geraniol, an isomer of geraniol with a terminal olefin bond. Apparently, the catalyst for the asymmetric hydrogenation also catalyzes the isomerization of geraniol to γ-geraniol. Although geraniol was the only substrate charged with the catalyst into the reactor, there were actually two different substrates present in the reactor prior to application of hydrogen to the reactor as a result of isomerization of geraniol during the catalyst dissolution period.

A terminal olefin would be hydrogenated at a much faster rate as compared with its internal olefin isomer. Hence, the first distinct kinetic regime in Fig. 11 resulted from rapid hydrogenation of γ-geraniol, and the second from hydrogenation of geraniol. These intriguing kinetics are also shown well in the concentration profiles in Fig. 13.

Even more intriguing is the fact that these two prochiral isomeric olefins underwent hydrogenation with respectively high enantioselectivities (ee $\sim 85\%$) to β-citronellol products of opposite absolute stereo configuration under these reaction conditions. The vast difference in the rate of hydrogenation and the opposite enantioselectiviy associated the hydrogenation of geraniol and γ-geraniol results in the "flip" of the
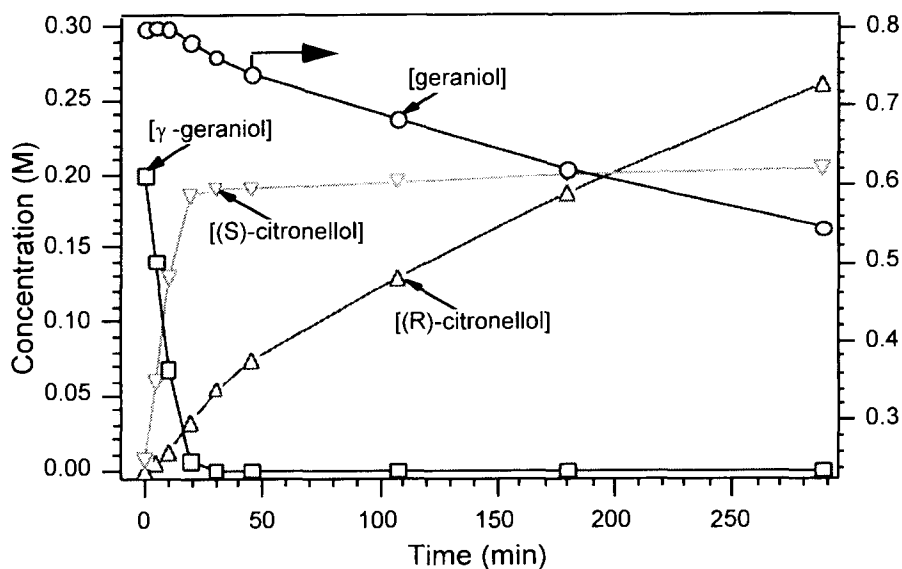

Fig. 13. Concentration profiles of components in the reactor during hydrogenation that corresponds to reaction described in Fig. 11. Note that prior to application of H_2, 20% of the geraniol charge into the reactor has isomerized to γ-geraniol.

incremental enantiomeric excess from 85% (R) to 85%(S), and consequently, the increase of the cumulative enantiomeric excess with the progress of the reaction (Fig. 12).

It is common practice in process development of synthetic organic reactions to take only one sample at the end of the reaction to determine the selectivity of the reaction. Should one have done so with this reaction, one would have concluded that the enantioselectivity of the catalyst for hydrogenation of geraniol under these conditions is poor (ee ~ 40%), while the fact of the matter is that the enantioselectivity is rather high (ee ~ 85%). More importantly, one would have missed the observation of presence of γ-geraniol, which is the key for understanding the underlying reasons for the observed inversion in the enantiomeric excess in Fig. 12. Observation of the unusual heat flow, however, prompts one to look more closely at the composition of components in the reactor, thus, revealing the isomerization-hydrogenation network.

4. Extracting kinetic parameters from the heat flow data

Equation 1 shows that under isothermal conditions, the heat flow rate is proportional to a summation of rate of concentration changes of the substrate and intermediates as weighed by their corresponding heats of reaction ΔH_i. A simple heat flow profile contains embedded in it information necessary to determine concentrations of all species involved in the reaction network, provided that valid kinetic expressions are used.

After a kinetic model that contains rate expressions for all steps is chosen, concentration profiles of all species in the reactor may be predicted following a fit of the calculated heat flow profile to the experimental profile by adjusting the ΔH_is and rate coefficients in the kinetic model. The ΔH_is may either be left as variables, in which case, the values from semi-empirical quantum mechanical methods may be used as initial guess, or values can be measured directly. In turn, one may use the extent of agreement between the predicted concentration profiles and the experimental ones to judge how valid the kinetic model is. In this manner, it is possible to extract from heat flow information rate coefficients associated with each step as well as concentration profiles of each species in the reactor in the reaction network.

Furthermore, by carrying out the reaction at different temperatures, rate coefficients as a function of temperature can be determined. Consequently, kinetic parameters such as activation energies and pre-exponential factors of rate coefficients associated with each step may be determined.

5. Conclusions

From a comparison between various methods of monitoring kinetics of complex chemical reactions, reaction calorimetry stands out as one of the most powerful tools for studying kinetics of chemical processes because it provides on-line, quasi-continuous, and non-invasive measures of reaction rate. The clear kinetic pictures revealed by the calorimetry offer telltale evidence about reaction pathways and mechanisms.

When combined with chemical analysis data, and/or hydrogen uptake rate data, in the case of hydrogenation reactions, the heat flow data yield stepwise thermodynamic information such as the heats of reaction associated with individual steps in consecutive reaction networks. As a result, heats of formation of even unstable intermediates can be determined. More importantly, these results help to discriminate between proposed pathways by comparing experimentally-determined heats of formation of the proposed intermediates with those calculated using semi-empirical quantum mechanical methods.

The heat flow data may also yield kinetic parameters associated with each individual steps because the simple heat flow curve contains embedded in it information necessary to determine concentrations of all species involved in the reaction network, provided that valid kinetic expressions are used. Thus, by modelling using a valid kinetic model, concentration profiles of all species in the reactor may be calculated. Conversely, how well the calculated concentration profiles compare with the measured ones can serve as a guide how valid the kinetic model is.

Acknowledgements

References

[1] For applications of the Mettler Reaction Calorimeter in process characterization and process development, see for example, Proceedings of the 6th RC User Forum.... USA, 1993.
[2] R. Landau, U.S. Singh, F. Gortsema, Y. -K. Sun, S.C. Gomoka, T. Lam, M. Futran and D.G. Blackmond, "A reaction calorimeter investigation of the hydrogenation of a substituted pyrazine," J. Cat. 157 (1995) 201.
[3] J. Wang, Y. -K. Sun, C. LeBlond, R.N. Landau and D.G. Blackmond, "Asymmetric hydrogenation of ethyl pyruvate over pt: relationship between conversion and enantioselectivity," J. Cat, 161 (1996) 752.
[4] Y.-K. Sun, J. Wang, C. LeBlond, R.N. Landau and D.G. Blackmond, "Asymmetric hydrogenation of ethyl pyruvate: diffusion effects on enantioselectivity," J. Cat. 161 (1996) 759.
[5] Y.-K. Sun, C. LeBlond, J. Wang, D.G. Blackmond, J. Laquidara and J.R. Sowa, Jr., "Observation of a $[RuCl_2((S)-(-)-tol-binap)] \cdot N(C_2H_5)_3$ catalyzed isomerization-hydrogenation network," J. Am. Chem. Soc. 117 (1995) 12647.
[6] R. Reamer, unpublished results.